Journal Name

COMMUNICATION

A new C,N-cyclometalated osmium(II) arene anticancer scaffold with a handle for functionalization and antioxidative properties

Received 00th January 20xx,
Accepted 00th January 20xx

DOI: 10.1039/x0xx00000x

www.rsc.org/

Enrique Ortega,[a] Jyoti G. Yellol,[a] Matthias Rothemund,[b] Francisco J. Ballester,[a] Venancio Rodríguez,[a] Gorakh Yellol,[a] Christoph Janiak,[c] Rainer Schobert[b] and José Ruiz [a,*]

A series of six osmium(II) complexes of the type [(η⁶-*p*-cymene)Os(C^N)X] (X = chlorido or acetato) containing benzimidazole C^N ligands with an ester group as a handle for further functionalization have been synthesized. They exhibit IC_{50} values in the low micromolar range in a panel of cisplatin (CDDP)-resistant cancer cells (approximately 10× more cytotoxic than CDDP in MCF-7), decrease levels of intracellular ROS and reduce NAD^+ coenzyme, and inhibit tubulin polymerization. This discovery could open the door to a new large family of osmium(II)-based bioconjugates with diverse modes of action.

Mechanistically, CDDP and carboplatin exert their anticancer activity through formation of platinum-DNA adducts, interfering with transcription, DNA replication and mitosis and thus leading to cell death.[1] However, due to issues of resistance and toxicity the development of new cancer treatments is crucial. In this way, an impressive amount of metal complexes has been explored as chemotherapeutic agents.[2] Thus the ruthenium(III) complex NKP-1339 undergoing clinical trials for cancer treatment,[3a] and Ru^{II}(η⁶-arene) complexes, which have been investigated for their tunability and novel modes of action.[3b-e] However, the 5d metal ion Os(II), the heavier congener of Ru(II), has received comparatively less attention as a chemotherapeutic agent,[4] and its clinical applicability for cancer treatment remains to be determined. The mechanism of action of osmium(II)-based anticancer agents *in vitro* often involves cell-cycle progression blockage and the induction of apoptosis through the generation of reactive oxygen species (ROS).[5] Interestingly, organometallic compounds can exhibit a distinctive ability to modulate the level of intracellular ROS, which are key signalling molecules within cancer cells associated with tight redox regulation and tumor progression.[6] While several metallodrugs have been described as ROS-generating agents that cause oxidative stress,[5,7] some examples of reduction of ROS have also been reported.[8–10] In fact, abrogating ROS signalling has been established as an effective strategy to inhibit cancer cell proliferation.[11]

We recently reported a series of half-sandwich "piano-stool" C,N-cyclometalated ruthenium(II) anticancer complexes bearing the benzimidazole pharmacophore with promising biologically activity,[12] and an octahedral benzimidazole iridium(III) conjugate to tumor-targeting vectors based on octreotide peptide.[13] Accordingly, in continued efforts of developing novel, better metallodrugs, here we disclose a series of organometallic osmium(II) complexes of the type [(η⁶-*p*-cymene)Os(C^N)X] (Fig. 1A) containing a 2-arylbenzimidazole C^N ligand which incorporates an ester group for further functionalization. They were synthesized using the generalized procedure shown in Fig. 1A. The corresponding benzimidazole ligand was treated with *p*-cymene osmium(II) dimer [(*p*-cymene)$OsCl_2]_2$ and sodium acetate to obtain the corresponding osmium complex (**1**–**6**) in moderate to good yield (47–68%), isolated as chlorido or acetato derivatives depending, probably, on the solubility of the monomer. The structures of the **1**–**6** were confirmed by ^{1}H and ^{13}C NMR, IR (Fig. S1-S15 in the ESI†) and ESI-MS spectrometry, elemental analysis and X-ray crystallography (for **1** and **6**).

In the ^{1}H NMR spectra of **1**-**6** the disappearance of one aromatic proton of the 2-arylbenzimidazole ligand was observed, and the arene protons of *p*-cymene exhibited four non-equivalent doublets. The presence for **5** and **6** of a singlet at 1.60 ppm was assigned to the methyl group of the acetato ligand. The positive ion ESI-MS spectra displayed the $[M - Cl]^+$ (for **1**–**4**) or $[M - OAc]^+$ (for **5** and **6**) peaks in methanolic solution with the expected isotopic distribution pattern.

The molecular structures of **1** and **6** are shown in Fig. 1B. Crystallographic data are listed in Table S4 for **1** and Table S5

[a] *Departamento de Química Inorgánica and Regional Campus of International Excellence "Campus Mare Nostrum", Universidad de Murcia, and Biomedical Research Institute of Murcia (IMIB-Arrixaca), E-30071 Murcia, Spain, Tel: + 34 868887455, Email: jruiz@um.es.*
[b] *Organic Chemistry Laboratory, University Bayreuth, Bayreuth, Universitaetsstrasse 30, D-95440, Germany*
[c] *Institut für Anorganische Chemie und Strukturchemie, Heinrich-Heine-Universität Düsseldorf, Universitätsstrasse 1, D-40225 Düsseldorf, Germany*

Electronic Supplementary Information (ESI) available: Synthesis, characterization data and biological study details. CCDC 1859533 (**1**) and 1859534 (**6**). For ESI and crystallographic data in CIF or other electronic format see DOI: 10.1039/x0xx00000x

Table 1 IC_{50} (μM) for **1**-**6** and CDDP after 48 h.[a] Resistance Factors are given in parentheses.

Complex	A2780	A2780cisR (RF)	MCF7	518A2	HCT116^{wt}	HCT116$^{[-/-]}$	EA.hy926	BGM
1	3.6 ± 0.7	3.4 ± 0.1 (0.9)	4.4 ± 0.1	6.1 ± 0.4	4.5 ± 0.1	5.5 ± 0.6	5.7 ± 0.2	14.2 ± 0.5
2	2.0 ± 0.2	1.8 ± 0.1 (0.9)	3.7 ± 0.1	4.8 ± 0.3	3.8 ± 0.4	3.6 ± 0.3	4.9 ± 0.6	9.8 ± 0.7
3	1.9 ± 0.1	1.89 ± 0.09 (1.0)	4.2 ± 0.1	4.8 ± 0.7	3.8 ± 0.2	4.6 ± 0.6	4.9 ± 0.2	11 ± 1
4	2.5 ± 0.5	3.0 ± 0.5 (1.2)	4.9 ± 0.1	4.1 ± 0.5	4.9 ± 0.2	3.8 ± 0.1	3.6 ± 0.2	7.6 ± 0.2
5	2.0 ± 0.1	3.7 ± 0.2 (1.9)	3.1 ± 0.2	6.9 ± 2.3	8.8 ± 0.8	6.9 ± 0.8	9.0 ± 1.0	7.6 ± 0.2
6	0.98 ± 0.03	1.0 ± 0.1 (1.0)	0.76 ± 0.03	3.1 ± 0.6	2.3 ± 0.2	2.9 ± 0.1	3.1 ± 0.1	1.7 ± 0.1
CDDP	1.5 ± 0.2	44 ± 4 (30.6)	47 ± 3	2.7 ± 0.2	10.3 ± 0.2	18.0 ± 1.8	5.7 ± 0.2	9.8 ± 0.4

[a] Cell viability was determined by the MTT assay after 48 h treatment and IC_{50} values were calculated as described in the Experimental Section. Each value represents the mean±SD of three independent experiments. Resistance factors are given in parentheses.

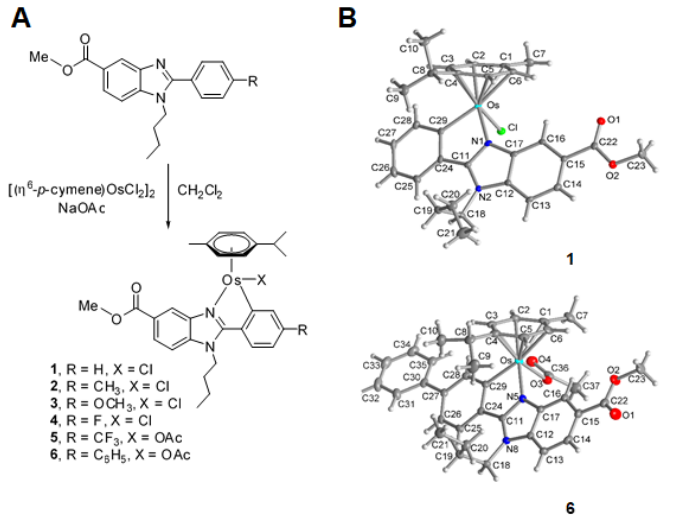

Fig. 1 Synthesis of complexes **1**–**6** (A). Molecular structures (B) with atom numbering schemes for **1** and **6** are shown with thermal ellipsoids at 50% probability level.

for **6** (ESI†). The osmium centers in **1** and **6** adopt a half-sandwich ''three-leg piano-stool'' geometry. The selected bond lengths and angles of **1** and **6** are listed in Table S6 for **1** and Table S7 for **6** (ESI†). The Os–chlorido bond length for **1** was found to be 2.4164 (9) Å, a typical value for organometallic Os complexes.[14] The Os–arene distance for **1** was larger than in **6** (1.714(1) and 1.680(1) Å, respectively). C···H and H···H close intermolecular contacts were the most important non-covalent intermolecular interactions for the packing of these complexes (see Fig. S32-S34, and Table S8 in the ESI†). There are no significant π·· π interactions.[9] Hydrolysis of the Os−X bond (X= Cl or OAc) is relatively rapid in MeOD-d_4/D_2O mixtures as observed by ^{1}H NMR (Fig. S16 and S17). Partial reversibility of the hydrolysis of **4** was observed when NaCl (4 mM) was added to the MeOD-d_4/D_2O solution (Fig. S16D). The HPLC chromatogram (Fig. S18) of **2** in RPMI culture medium (which contains a high concentration of salts) remains unaltered after 24 h, the ESI-MS spectrum displaying the $[M - Cl]^+$ peaks.

The antiproliferative activities of the six osmium compounds containing a butyl group attached to the benzimidazole C^N ligand and a handle for functionalization were evaluated in a panel of human cancer cell lines, including cells of the epithelial ovarian carcinoma A2780, CDDP-resistant ovarian cancer A2780cisR, breast cancer MCF7, 518A2 melanoma, colon carcinoma HCCT116^{wt} (wildtype), colon carcinoma HCCT116$^{-/-}$ (p53 knock-out mutant), and also in the non-tumorigenic human endothelial hybrid cells EA.hy926 and the Buffalo green monkey cells BGM. For comparison, CDDP cytotoxicity was also evaluated. All Os compounds exhibited high antiproliferative activities against the studied cancer cell lines with IC_{50} values in the low micromolar range (see Table 1) and they were able to overcome the acquired resistance to CDDP in the A2780cisR cell line (Table 1). Their resistance factors (RFs) were much lower than that of CDDP (values below 2 *vs* 30),[9] suggesting that their mode of action is different from that of CDDP. On the other hand, a slight reduction of the anticancer activity towards the multidrug resistant MCF-7, the highly metastatic 518A2 and HCT116^{wt} in respect to A2780 was observed. It is worth noting that **1**–**6** proved markedly more cytotoxic than CDDP (>40 μM) in MCF-7 (10–60-fold) which is inherently resistant to CDDP. Likewise, of interest are the similar IC_{50} values obtained in both wildtype HCCT116^{wt} and p53 knock-out HCT116$^{-/-}$colon carcinoma cells, which suggests that molecular mechanisms underlying cell death induction by the Os complexes might be p53-independent. In addition to this, the *in vitro* antiproliferative activity was evaluated against the non-tumorigenic EA.hy926 and BGM cell lines to determine the differential selectivity for tumor cells. The toxicity of the complexes was found to be comparable to that of CDDP with a slightly higher cytotoxicity against cancer cells. Overall, **2** and **3** were the most potent agents with the higher selectivity factor (SF) values in all tested cancer cell lines (Tables S1 and S2 in the ESI†). Cellular concentrations of metals in A2780 cells having been exposed to **2**, **3** or CDDP for 24 h were determined by ICP-MS in order to investigate the relationship between cellular uptake and cytotoxicity. The results (Fig. S28) indicate that cellular uptake of both **2** and **3** is similar and 10-fold higher than that of Pt. In addition, the amount of osmium bound to DNA in A2780 cells (as measured by ICP-MS) was below 1 pg Os/μg DNA, suggesting that DNA is not likely to be the main target of the present complexes (Table S3 in ESI†).[16] The ability of **2** and **3** to induce apoptosis in A2780 cells was also evaluated. As shown in Fig. 2A, complexes **2** and **3**

considerably increased the percentage of early apoptotic cells (Annexin V^+/PI^-) following 48 h treatment with respect to controls whereas the necrotic population (Annexin V^-/PI^+) shows no significant increase. In contrast, the most cytotoxic complex **6** (Fig. S22 in ESI†) contributed to necrotic cell death rather than apoptosis induction, which could explain its lack of selectivity for cancer cells.

Then we explored the ability of the osmium complexes to intervene in reduction of nicotinamide adenine nucleotide (NAD^+) to NADH as this redox pair is involved in relevant redox signalling pathways within cells.[15] The catalytic formation of NADH was monitored by UV-Vis measuring the UV absorption of NADH at 339 nm (Fig. S19-S21 in ESI†). For both complexes **2** and **3** an increase in intensity of the NADH absorption was observed. The turnover frequency reached a maximum of 9 and 10 at 4 h for **2** and **3**, respectively.

Next, we investigated the intracellular ROS levels after treatment of A2780 cells with Os complexes, detected using 2'7'-dichlorodihydrofluorescein diacetate (DCFH-DA) staining. DCFH-DA is converted to the fluorescent product 2',7'-dichlorofluorescein (DCF) by ROS. As shown in Fig. 2B, the DCF fluorescence intensity underwent a dose-dependent decrease upon treatment with **2** and **3** when compared to CDDP at 24 h. In addition to this, levels of ROS were monitored by a DCFH-DA assay corroborating the antioxidant properties of **2**, which induced a reduction of ROS of up to 20% in 2 h (Fig. S25 and S26 in ESI†). ROS are not *by-products* of cellular metabolism but rather key signalling molecules intervening in cancer proliferation pathways.[11] Although several organometallic compounds have been described as generators of ROS,[5-7] other complexes are known to induce cell death by reductive stress.[8-10,17] In this study, we showed that the addition of **2** or **3** caused a decrease of the ROS level below the threshold that cancer cells require for survival probably due to disruption of multiple intracellular redox reactions. On the other hand, mitochondrial membrane potential (MMP) disruption is involved in the mode of action of numerous organometallic anticancer compounds.[7a,18,19] The treatment of A2780 cells with **2** or **3** did not lead to a significant reduction of fluorescence of the MMP integrity indicator, Rhodamine-123 dye, compared to untreated controls (Fig. S23 and S24 in ESI†). To further characterize the cytotoxic effect of our Os complexes, A2780 cells were treated with **2**, **3** or CDDP for 24 h and analyzed by flow cytometry using propidium iodide staining. CDDP induces cell cycle arrests at S and G_2 phases according to previous reports.[7a] However, the modulation of the cell cycle of A2780 cells upon treatment with **2** or **3** differed from that of cells treated with CDDP (Fig. 2C). In fact, **2** and **3** caused a dose-dependent G_0/G_1 arrest with minor effects on S or G_2/M phases. These results indicate an activation of cell cycle blockage in response to cellular oxidative status imbalance as G_1 arrest has been associated with low ROS levels.[20]

The lack of MMP disturbance and the induced decrease in ROS levels upon cell treatment ruled out ROS-mediated mitochondrial dysfunction as a trigger for cell death. However,

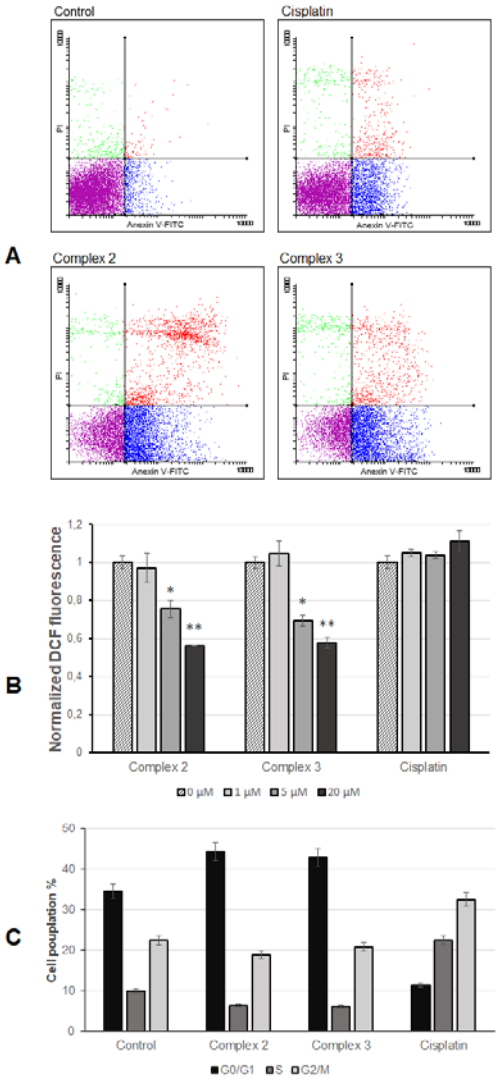

Fig. 2 Apoptosis inducing effects of **2** and **3** after 48 h treatment of A2780 cells at final equitoxic concentrations determined by flow cytometry (A). ROS levels induced by **2** and **3** after 24 h (B). Cell cycle analysis of A2780 cells treated with **2**, **3** or CDDP for 24 h (C). Experiments were performed in triplicate, *p < 0.05, **p <0.01, two-tailed Student's t-test.

flow cytometry experiments confirmed apoptosis and cell cycle arrest as the mechanism of cell death induction. Rather, the ability of **2** and **3** to effectively participate in reduction of NAD^+ to NADH together with the depletion of intracellular ROS levels indicated a shift in the intracellular redox balance toward a reductive stress environment where several metabolic reactions could be impaired, thus causing a selective arrest in progression from G_0/G_1 to S phase which probably triggered the apoptotic program. Moreover, **2** and **3** inhibited the *in vitro* tubulin polymerization (Fig. 3). Both tested compounds reduced the polymerization rate of the tubulin as well as the maximum OD_{340} after 90 minutes of incubation in comparison to the control with the solvent, though none of the complexes were able to reach the activity of colchicine at this concentration.

In conclusion, a series of C,N-cyclometalated osmium arene

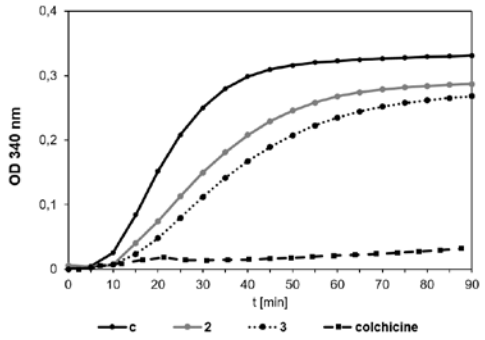

Fig. 3 Effects on the *in* vitro tubulin polymerization by 10 μM of **2**, **3** and colchicine as control, determined by OD measurement at 340 nm over 90 minutes at 37 °C.

complexes [(η^6-*p*-cymene)Os(C^N)X] (X = chlorido or acetato) containing benzimidazole C^N ligands with an ester group as a handle for further functionalization has been prepared with high antiproliferative activities against various cancer cell lines including CDDP-resistant cancer cells. Further biological studies showed that complexes **2** and **3** exhibited antioxidative properties by decreasing levels of intracellular ROS and reducing NAD^+ coenzyme, and that they disturbed the cell cycle progression at the G_0/G_1 phase and caused apoptotic cell death in a p53-independent mode of action. These preliminary results could open the door to a new large family of Os(II)-based bioconjugates with diverse and simultaneous functions through an amide (or ester) bond formation with the uncoordinated carboxyl group easily obtainable by hydrolysis.

This work was supported by the Spanish Ministry of Economy and Competitiveness and FEDER funds (Project CTQ2015-64319-R). F.B. thanks Fundación Séneca-CARM (Project 20277/FPI/17). The authors also thank the members of the COST Action CM1105 for stimulating discussions.

Conflicts of interest

There are no conflicts to declare

Notes and references

1 (a) D. Wang and S. J. Lippard, *Nat. Rev. Drug Discov.*, 2005, **4**, 307–320.; (b) E. R. Jamieson and S. J. Lippard, *Chem. Rev.*, 1999, **99**, 2467–2498.

2 (a) T.-S. Kang, Z. Mao, C.-T. Ng, M. Wang, W. Wang, C. Wang, S. M.-Y. Lee, Y. Wang, C.-H. Leung and D.-L. Ma, *J. Med. Chem.*, 2016, **59**, 4026–4031; (b) A. Johnson, I. Marzo and M. C. Gimeno, *Chem. – Eur. J.*, 2018, **24**, 11693–11702; (c) S. Mena, A. Mirats, A. B. Caballero, G. Guirado, L. A. Barrios, S. J. Teat, L. Rodriguez-Santiago, M. Sodupe and P. Gamez, *Chem. – Eur. J.*, 2018, **24**, 5153–5162; (d) J. Fernández-Gallardo, B. T. Elie, T. Sadhukha, S. Prabha, M. Sanaú, S. A. Rotenberg, J. W. Ramos and M. Contel, *Chem. Sci.*, 2015, **6**, 5269–5283.

3 (a) R. Trondl, P. Heffeter, C. R. Kowol, M. A. Jakupec, W. Berger and B. K. Keppler, *Chem. Sci.*, 2014, **5**, 2925–2932; (b) A. L. Noffke, A. Habtemariam, A. M. Pizarro and P. J. Sadler, *Chem. Commun.*, 2012, **48**, 5219–5246; (c) C. G. Hartinger, N. Metzler-Nolte and P. J. Dyson, *Organometallics*, 2012, **31**, 5677–568; (d) B. S. Murray, M. V. Babak, C. G. Hartinger and P. J. Dyson, *Coord. Chem. Rev.*, 2016, **306**, 86–114; (e) G. S. Yellol, A. Donaire, J. G. Yellol, V. Vasylyeva, C. Janiak and J. Ruiz, *Chem. Commun.*, 2013, **49**, 11533–11535.

4 (a) M. Hanif, A.A. Nazarov, C.G. Hartinger, W. Kandioller, M. A. Jakupec, V. B. Arion, Paul J. Dyson and B. K. Keppler, *Dalton Trans.*, 2010, **39**, 7345-7352; (b) A. F. A. Peacock and P. J. Sadler, *Chem. Asian J.* 2008, **3**, 1890-1899; (c) J. P. C. Coverdale, I. Romero-Canelón, C. Sanchez-Cano, G. J. Clarkson, A. Habtemariam, M. Wills and P. J. Sadler *Nat. Chem.*, 2018, **10**, 347–354; (d) P. Zhang, Y. Wang, K. Qiu, Z. Zhao, R. Hu, C. He, Q. Zhang and H. Chao, *Chem. Commun*. 2017, **53**, 12341-12344.

5 (a) R. J. Needham, C. Sanchez-Cano, X. Zhang, I. Romero-Canelón, A. Habtemariam, M. S. Cooper, L. Meszaros, G. J. Clarkson, P. J. Blower and P. J. Sadler, *Angew. Chem. Int. Ed Engl.*, 2017, **56**, 1017–1020; (b) J. M. Hearn, I. Romero-Canelón, A. F. Munro, Y. Fu, A. M. Pizarro, M. J. Garnett, U. McDermott, N. O. Carragher and P. J. Sadler, *Proc. Natl. Acad. Sci. U. S. A.*, 2015, **112**, E3800-3805; (c) I. Romero-Canelon, M. Mos and P.J. Sadler, *J. Med. Chem.*, 2015, **58**, 7874–7880.

6 (a) U. Jungwirth, C. R. Kowol, B. K. Keppler, C. G. Hartinger, W. Berger and P. Heffeter, *Antioxid. Redox Signal.*, 2011, **15**, 1085–1127; (b) C. Gaiddon and M. Pfeffer, *Eur. J. Inorg. Chem.*, 2017, 1639–1654; (c) R. McCall, M. Miles, P. Lascuna, B. Burney, Z. Patel, K. J. Sidoran, V. Sittaramane, J. Kocerha, D. A. Grossie, J. L. Sessler, K. Arumugam and J. F. Arambula, Chem. Sci., 2017, **8**, 5918–5929; (d) D. A. Megger, K. Rosowski, C. Radunsky, J. Kösters, B. Sitek and J. Müller, Dalton Trans., 2017, **46**, 4759–4767; (e) D. Tolan, V. Gandin, L. Morrison, A. El-Nahas, C. Marzano, D. Montagner and A. Erxleben, Sci. Rep., 2016, 6, 29367; (f) J.-J. Zhang, J. K. Muenzner, M. A. Abu el Maaty, B. Karge, R. Schobert, S. Wölfl and I. Ott, Dalton Trans., 2016, 45, 13161–13168.

7 (a) V. Novohradsky, J. Yellol, O. Stuchlikova, M.D. Santana, H. Kostrhunova, G. Yellol, J. Kasparkova, D. Bautista, J. Ruiz and V. Brabec, *Chem. Eur. J.*, 2017, **23**, 15294–15299; (b) J.-J. Cao, C.-P. Tan, M.-H. Chen, N. Wu, D.-Y. Yao, X.-G. Liu, L.-N. Jia and Z.-W. Mao, *Chem Sci.*, 2017, **8**, 631–640.

8 C. A. Riedl, M. Hejl, M. H. M. Klose, A. Roller, M. A. Jakupec, W. Kandioller and B. K. Keppler, *Dalton Trans.*, 2018, **47**, 4625–4638.

9 A. Zamora, S. A. Pérez, M. Rothemund, V. Rodríguez, R. Schobert, C. Janiak and J. Ruiz, *Chem. Eur. J.*, 2017, **23**, 5614.

10 M. Schmidlehner, L. S. Flocke, A. Roller, M. Hejl, M. A. Jakupec, W. Kandioller and B. K. Keppler, *Dalton Trans.*, 2016, **45**, 724–733.

11 D. Trachootham, J. Alexandre and P. Huang, *Nat. Rev. Drug Discov.*, 2009, **8**, 579–591.

12 J. Yellol, S. A. Pérez, A. Buceta, G. Yellol, A. Donaire, P. Szumlas, P. J. Bednarski, G. Makhloufi, C. Janiak, A. Espinosa and J. Ruiz, *J. Med. Chem.*, 2015, **58**, 7310–7327.

13 V. Novohradsky, A. Zamora, A. Gandioso, V. Brabec, J. Ruiz and V. Marchán, *Chem. Commun.*, 2017, **53**, 5523-5526.

14 C. A. Riedl, L. S. Flocke, M. Hejl, A. Roller, M. H. M. Klose, M.A. Jakupec, W. Kandioller and B. K. Keppler, *Inorg. Chem.*, 2017, **56**, 528–541.

15 A. McSkimming and S. B. Colbran, *Chem. Soc. Rev.*, 2013, **42**, 5439–5488.

16 J. Yellol, S. A. Pérez, G. Yellol, J. Zajac, A. Donaire, G. Vigueras, V. Novohradsky, C. Janiak, V. Brabec and J. Ruiz, *Chem. Commun.*, 2016, **52**, 14165-14168.

17 J. J. Soldevila-Barreda, I. Romero-Canelón, A. Habtemariam and P. J. Sadler, *Nat. Commun.*, 2015, **6**, 6582.

18 F.-X. Wang, M.-H. Chen, X.-Y. Hu, R.-R. Ye, C.-P. Tan, L.-N. Ji and Z.-W. Mao, *Sci. Rep.*, 2016, **6**, 38954.

19 D. Wan, B. Tang, Y.-J. Wang, B.-H. Guo, H. Yin, Q.-Y. Yi and Y.-J. Liu, *Eur. J. Med. Chem.*, 2017, **139**, 180–190.

20 C. G. Havens, A. Ho, N. Yoshioka and S. F. Dowdy, *Mol. Cell. Biol.*, 2006, **26**, 4701–4711.

